Carbohydrate Polymers 277 (2022) 118886

Contents lists available at ScienceDirect

Carbohydrate Polymers

journal homepage: www.elsevier.com/locate/carbpol

Regioselective synthesis of polysaccharide–amino acid ester conjugates

Yang Zhou [a], Kevin J. Edgar [a,b,*]

[a] Department of Sustainable Biomaterials, Virginia Tech, Blacksburg, VA 24061, United States
[b] Macromolecules Innovation Institute, Virginia Tech, Blacksburg, VA 24061, United States

ARTICLE INFO

Keywords:
Copolymers
Polysaccharide-amino acid ester conjugates
Regioselectivity
Cellulose
Dextran
Chemoselectivity

ABSTRACT

Site-specific conjugation of polysaccharides with proteins is very challenging. Creating the ability to control chemo- and regioselective reaction between polysaccharides and amino acid derivatives can not only create potentially useful and bioactive natural polymer constructs, but should also provide useful guidance for the principles of polysaccharide–protein conjugate synthesis. In this work, we exploited regioselective bromination of the non-reducing end primary dextran hydroxyl using *N*-bromosuccinimide (NBS) and triphenylphosphine (Ph_3P) in the dimethylacetamide (DMAc) and lithium bromide solvent system, thereby enabling a regio- and chemoselective synthetic strategic approach to a variety of polysaccharide-amino acid ester adducts. We demonstrated selective condensation of the α-amino groups of esters of the amino acids tyrosine and proline, displacing the single, terminal C6 bromides of 6-BrDextran, as well as the 6-Br moieties of 6-BrCA320S, with high conversion (71–96%). Histidine ester side group amines were found to react with 6-BrCA320S, while those of tryptophan ester did not. These results provide useful access to polysaccharide–amino acid ester adducts of various architectures, and guide us in designing new pathways to polysaccharide–protein copolymers.

1. Introduction

Both research and commercial interest in protein drugs have been on the rise, due to their higher specificity, faster onset of action, and lower required doses compared to conventional small molecule therapeutics (Damodaran & Fee, 2010). However, efficacy of first-generation protein drugs is often limited by inherent issues, including those related to stability, solubility, short elimination half-lives, immunogenicity, and toxicity (Jevševar et al., 2010). PEGylation is a strategy that has proved clinically effective by shielding the protein, increasing its apparent size, and protecting against metabolic destruction (Roberts et al., 2012). PEGylated proteins may, however, accumulate within cells and cause vacuolization due to inadequate biodegradation of high molecular weight polyethylene glycol (PEG) (Baumann et al., 2014; Kawai, 2005). Conjugation of a biodegradable polysaccharide to the protein drug is another promising strategy, one of particular promise given the fact that many polysaccharides are biodegradable, have low toxicity, and do not typically provoke a strong immune response *in vivo*. However, most common methods for synthesis of polysaccharide–protein conjugates are not regioselective, including reductive amination, Maillard reaction, 1-ethyl-3-(3-dimethylaminopropyl) carbodiimide/*N*-hydroxysuccinimide (EDC/NHS) coupling, 4-(4,6-dimethoxy-1,3,5-triazin-2-yl)-4-methylmorpholinium chloride (DMTMM) coupling, and disulfide bond formation (Zhou et al., 2021). These rather non-specific conjugation methods afford structurally non-uniform polysaccharide–protein conjugates, which may lead to failure during clinical trials and/or regulatory approval processes (Ferguson et al., 2020). Therefore, control of the site of conjugation would be highly favorable for successful development of useful polysaccharide–protein conjugates.

Amino acids, both unprotected and *tert*-butyl oxycarbonyl (Boc)-protected, and amino acid esters have been studied as model compounds for protein–polysaccharide conjugation. In one method, investigators first regioselectively oxidized the primary 6-OH groups of cellulose, then condensed these to form amide linkages with amino acids or their derivatives via EDC/NHS coupling (Huang et al., 2013; Pahlevan et al., 2018). However, the polysaccharide may contain residual C6 aldehyde groups even after long reaction times because of incomplete oxidation, likely due in part to acetal and/or hemiacetal formation with polysaccharide hydroxyls (Saito & Isogai, 2004). These unreacted aldehyde groups create the possibility of undesired (and potentially toxic) side reactions. Maillard reaction between the amino acid and the polysaccharide reducing end, which is in equilibrium between hemiacetal and ring-opened aldehyde forms, can afford effective control of the polysaccharide conjugation site (Sun et al., 2018; Yi et al., 2019).

* Corresponding author at: Department of Sustainable Biomaterials, Virginia Tech, Blacksburg, VA, 24061, United States.
E-mail address: kjedgar@vt.edu (K.J. Edgar).

https://doi.org/10.1016/j.carbpol.2021.118886
Received 1 October 2021; Received in revised form 2 November 2021; Accepted 9 November 2021
Available online 13 November 2021
0144-8617/

However, there is typically only one reducing end per polysaccharide chain, meaning that this is not a route to conjugates with high degrees of substitution. It is also difficult to control the extent and chemoselectivity of the Maillard reaction. Further reactions of the initial conjugates can result in complex products which are difficult to analyze. Some downstream Maillard products may be toxic, causing issues including oxidative stress and inflammation *in vivo* (Zhou et al., 2021). Esterification of polysaccharide hydroxyls using Boc-protected amino acids (Hotzel et al., 2019; Zink et al., 2019), and EDC/NHS coupling of amino acids with carboxymethyl cellulose (Gürer et al., 2021) have been reported, but they are not regioselective methods.

Furuhata et al. reported a method for regioselective bromination of cellulose using *N*-bromosuccinimide (NBS) and triphenylphosphine (Ph_3P) in the dimethylacetamide (DMAc) and LiBr solvent system (Furuhata et al., 1992). The Edgar group has exploited this regioselective bromination to modify C6 polysaccharide hydroxyls and generate useful materials, including those from microcrystalline cellulose (in DMAc/LiBr) (Fox & Edgar, 2012), cellulose esters (in DMAc) (Liu & Edgar, 2017), curdlan (in DMAc/LiBr) (Zhang et al., 2017), pullulan (in *N*, *N*-dimethylformamide (DMF)/LiBr) (Pereira & Edgar, 2014), and dextran (in dimethyl sulfoxide (DMSO)) (Chen et al., 2020). Recently, the Edgar group reported regioselective chlorination of polysaccharides at the primary hydroxyl groups using methanesulfonyl chloride in DMF; this method employs less expensive reagents and has the significant benefit that it does not generate triphenylphosphine oxide, which can be difficult to remove quantitatively from the polysaccharide product (Gao et al., 2018).

We hypothesize that we can begin with regioselectively brominated cellulose acetate or dextran, then conjugate amino acid esters to the polysaccharide via nucleophilic displacement of the primary bromides, thereby affording regioselectively (or regiospecifically) substituted conjugates. The 6-Br groups of the brominated polysaccharide would be nucleophilically displaced by the α-amine moieties of the amino acid; some competition from other amine moieties where pertinent (e.g. of histidine) may also occur. We selected cellulose acetate and dextran as useful and illustrative starting polysaccharides. Cellulose acetates are the most important commercial esters of cellulose (Touati & Tadeo, 2017); they can be processed thermally or in solution, are (at the right DS) biodegradable (Buchanan et al., 1993), and are of interest for applications including wound dressings, tissue engineering scaffolds, transdermal delivery systems, and postsurgical devices (Khoshnevisan et al., 2018). 6-Brominated cellulose acetate will provide an illustrative and potentially useful example of a polysaccharide decorated in multiple, selective branch locations with an amino acid. Dextran is a hydrophilic, non-immunogenic polysaccharide composed of α-1,6-linked D-glucopyranose; it can be branched with α-linked glucose moieties from any of its secondary hydroxyl groups, depending on the bacterium that produces that particular dextran (Naessens et al., 2005). Linear (essentially unbranched) dextran is of particular interest in biomedical applications, including in drug delivery systems, since it has long been used in the clinic in intravenous infusions, in part due to its ability to promote osmotic balance (Heinze et al., 2006; Hu et al., 2021). In drug delivery, it has been valued for many reasons, including its capability to increase blood circulation time, and to reduce the toxicity and side effects of encapsulated drugs (Huang & Huang, 2019; Varshosaz, 2012). For the amino acid nucleophile, we chose to use amino acid esters in this initial study, to avoid complications due to insolubility or undesired reactivity of the natural amino acid zwitterion. We studied esters of several common amino acids, including those of tyrosine, proline, histidine, and tryptophan. This group of amino acid esters should provide guidance as to potential competition between the α-amino and (where pertinent) side chain amines of amino acids. Overall, we expected that these reaction partners would test our hypothesis and potentially prove the concept of this strategy, while providing initial guidance about any potential limitations.

2. Experimental

2.1. Materials

Cellulose acetate (CA320S, Eastman Chemical, DS(Ac) 1.78, DS(6-OH) 0.49, *M*w = 47.6 kDa (Liu & Edgar, 2017)) and dextran from *Leuconostoc mesenteroides* (Sigma-Aldrich, M_n 10,100 g/mol, determined by aqueous SEC (Chen et al., 2020)) were dried under vacuum at 50 °C overnight before use. Lithium bromide (Fisher) was dried under vacuum at 130 °C overnight before use. *N*-Bromosuccinimide (NBS, 99%, Sigma-Aldrich), triphenylphosphine (Ph_3P, 99%, Sigma-Aldrich), sodium iodide (Fisher), L-tyrosine methyl ester (98%, Sigma-Aldrich), L-tyrosine *tert*-butyl ester (99%, Sigma-Aldrich), L-proline *tert*-butyl ester (98%, Sigma-Aldrich), N_α-methoxycarbonyl-L-tryptophan methyl ester (98%, Sigma-Aldrich) and N_α, N_{im}-di-Boc-L-histidine methyl ester (97%, Sigma-Aldrich) were used as received. DMF (99.8%, Acros), DMAc (99.8%, Sigma-Aldrich), and DMSO (99.9%, Alfa Aesar) were kept over 4 Å molecular sieves. Regenerated cellulose dialysis tubing (molecular weight cut-off (MWCO) 3500 g/mol, Fisher) was used as received.

2.2. Measurements

^{1}H and ^{13}C NMR spectra were obtained on Agilent U4-DD2 400 MHz and Bruker Avance II 500 MHz instruments in DMSO-d_6 (trifluoroacetic acid (TFA) was added for ^{1}H NMR test, if no special instructions) at room temperature, using 256 scans for ^{1}H NMR and 10,000 scans for ^{13}C NMR spectra. Elemental analysis (EA) was performed by Midwest Microlab. Yields and DS values determined by ^{1}H NMR and elemental analysis were calculated according to the following equations:

Yield of products:

$$\%\text{Yield} = \frac{\text{moles of product}}{\text{moles of reactant}} \tag{1}$$

We assume 100% conversion on bromination of dextran.

$$\text{DS}_{\text{Ac}} = \frac{7 \times \text{I}(\text{AcCH}_3)}{3 \times \text{I}(\text{backbone})} \tag{2}$$

I is integral. DS_{Ac} is the DS of acetyl group. $AcCH_3$ is acetyl methyl group. There are 7 protons in the cellulose AGU and 3 protons in the acetyl methyl group.

$$\frac{\text{I}(\text{d}+\text{e})}{\text{I}(\text{backbone}+\text{a}+\text{b}+\text{c})} = \frac{4 \times \text{DS}_{\text{Tyr}}}{6 \times \text{DS}_{\text{Tyr}} + 7} \tag{3}$$

Letters correspond to those in Fig. 1. I is integral. DS_{Tyr} is the DS of tyrosine ester. There are 7 protons in the cellulose AGU; 4 protons in d and e; and 6 protons in a, b, and c.

$$\frac{\text{I}(\text{a})}{\text{I}(\text{backbone}+\text{b}+\text{e})} = \frac{9 \times \text{DS}_{\text{Pro}}}{3 \times \text{DS}_{\text{Pro}} + 7} \tag{4}$$

Letters correspond to those in Fig. S2. I is integral. DS_{Pro} is the DS of proline ester. There are 7 protons in the cellulose AGU; 9 protons in a; and 3 protons in b and e.

$$\frac{\text{I}(\text{a})}{\text{I}(\text{backbone}+\text{b}+\text{c}+\text{d})} = \frac{9 \times \text{DS}_{\text{His}}}{6 \times \text{DS}_{\text{His}} + 7} \tag{5}$$

Letters correspond to those in Fig. S3. I is integral. DS_{His} is the DS of histidine ester. There are 7 protons in the cellulose AGU; 9 protons in a; and 6 protons in b, c and d.

$$\frac{\text{I}(\text{a})}{\text{I}(\text{H1})} = \frac{9 \times \text{DS}_{\text{Tyr}}}{1} \tag{6}$$

Letters correspond to those in Fig. 5. I is integral. There are 9 protons in a and 1 proton in H1.

$$\frac{\text{I}(\text{a})}{\text{I}(\text{H1})} = \frac{9 \times \text{DS}_{\text{Pro}}}{1} \tag{7}$$

Letters correspond to those in Fig. 6. I is integral. There are 9 protons in a and 1 proton in H1.

$$DS_{Br} = \frac{\frac{\%Br}{79.90}}{\frac{\%C}{12.01} \Big/ (6 + 2 \times DS_{Ac})} \quad (8)$$

%Br and %C are the percentages of bromine and carbon measured by elemental analysis. DS_{Ac} is measured by ^{1}H NMR by Eq. (2). Any residual DMF should be substracted before using this equation. There are 6 carbons in the cellulose AGU and 2 carbons in the acetyl group.

$$DS_{Amino\ acid\ ester} = \frac{\left(\frac{\%N}{14.01}\right) \Big/ n(N)}{\frac{\%C}{12.01} - \left(\frac{\%N}{14.01}\right) \Big/ n(N) \times n(C) \Big/ 6 + 2 \times DS_{Ac}} \quad (9)$$

%N and %C are the percentages of nitrogen and carbon measured by elemental analysis. DS_{Ac} is measured by ^{1}H NMR by Eq. (2). n(N) and n(C) are the numbers of nitrogen atoms and carbon atoms, respectively, in the amino acid ester. There are 6 carbons in the cellulose AGU and 2 carbons in the acetyl group.

2.2.1. Regioselective bromination of CA320S

This method is modified from (Liu & Edgar, 2017). Cellulose acetate (CA320S, 4.00 g, 16.89 mmol) was dissolved in 160 mL DMAc in a 500 mL flask. Ph_3P (13.28 g, 50.63 mmol, 3 equiv per AGU) and NBS (9.00 g, 50.56 mmol, 3 equiv per AGU) were dissolved in separate 40 mL portions of DMAc. The Ph_3P solution was added to the 500 mL flask dropwise with stirring, followed by dropwise addition of the NBS solution. The solution was heated to 70 °C under N_2 for 1 h with stirring. After cooling to room temperature, the reaction mixture was poured into 4 L 50% aqueous methanol to precipitate the crude product. The precipitate was collected, and then redissolved in acetone, followed by reprecipitation in ethanol. This reprecipitation was carried out a second time. The precipitate was dried overnight at 60 °C in a vacuum oven to obtain 6-BrCA320S as a light brown fibrous material. Yield: 2.42 g, 9.07 mmol, 54%. ^{13}C NMR (500 MHz, DMSO-d_6) 20.7 (O–(C=O)–$\underline{C}H_3$), 33.3 ($\underline{C6}$–Br), 62.5 ($\underline{C6}$–O–(C=O)–CH_3), 69.0–81.5 ($\underline{C2}$, $\underline{C3}$, $\underline{C4}$, $\underline{C5}$), 99.3 and 102.8 ($\underline{C1}$), 168.0–170.0 (O–($\underline{C}$=O)–CH_3). Elemental analysis: C 43.35%, H 4.98%, N 0.35%, Br 14.02%; theoretical (DS(Ac) 1.78, DS(Br) 0.47): C 43.08%, H 4.95%, N 0, Br 14.09%.

2.2.2. Regioselective bromination of dextran

In a 100 mL round-bottom flask, dextran (1 g, 6.17 mmol) and LiBr (1 g, 11.52 mmol, 116 equiv per chain, 14.1 equiv per non-reducing end hydroxyl) were added to DMAc (20 mL), then stirred at 70 °C under N_2 for 1 h to get a clear solution, which was then cooled to room temperature. Ph_3P (2.62 g, 9.99 mmol, 101 equiv per chain, 12.3 equiv per non-reducing end hydroxyl) and NBS (1.78 g, 10.00 mmol, 101 equiv per chain, 12.3 equiv per non-reducing end hydroxyl) were dissolved in separate 10 mL portions of DMAc. The Ph_3P solution was added to the flask dropwise with stirring, followed by dropwise addition of the NBS solution. The solution was heated to 70 °C under N_2 for 2 h with stirring. The cooled solution was poured into 300 mL acetone to precipitate the product, which was collected by decantation and then washed twice with 300 mL portions of acetone. The precipitate was dialyzed against 80% acetone and DI-water in sequence, then the sequence was repeated, for 9 days in total. The mixture was freeze-dried to yield 6-BrDextran as a brown fibrous material. Yield: 336 mg, 1.98 mmol, 32%. ^{1}H NMR (500 MHz, DMSO-d_6) 3.00–4.14 ($\underline{H2\text{-}H6}$), 4.54–5.11 ($\underline{H1}$).

2.2.3. Synthesis of 6-tyrosine methyl ester-substituted cellulose acetate (6-TyrCA320S)

In a 100 mL round-bottom flask, 6-BrCA320S (200 mg, 0.75 mmol) was dissolved in 10 mL DMSO. Tyrosine methyl ester (2.20 g, 11.27 mmol, 15 equiv per AGU) and sodium iodide (225 mg, 1.50 mmol, 2 equiv per AGU) were added to the flask. The solution was kept at 80 °C with stirring for 48 h under N_2. The cooled solution was dialyzed against acetone for 7 days, then against DI-water for 2 days. The mixture was freeze-dried to yield the product as light yellow powder, 6-TyrCA320S. Yield: 192 mg, 0.62 mmol, 83%. ^{1}H NMR (400 MHz, DMSO-d_6) 2.02 (O–(C=O)–$\underline{CH_3}$), 2.73–5.30 (cellulose backbone, HO–Ph–CH_2–CH(–NH–C6)–(C=O)–O–$\underline{CH_3}$, HO–Ph–CH_2–$\underline{CH}$(–NH–C6)–(C=O)–O–CH_3, and HO–Ph–$\underline{CH_2}$–CH(–NH–C6)–(C=O)–O–CH_3), 6.71 and 6.98 (HO–$\underline{Ph}$–CH_2–CH(–NH–C6)–(C=O)–O–CH_3). ^{13}C NMR (500 MHz, DMSO-d_6) 20.6 (O–(C=O)–$\underline{CH_3}$), 38.3 (HO–Ph–$\underline{CH_2}$–CH(–NH–C6)–(C=O)–O–CH_3), 46.4 ($\underline{C6}$–NH), 51.3 (HO–Ph–$\underline{CH_2}$–CH(–NH–C6)–(C=O)–O–$\underline{CH_3}$), 62.7 ($\underline{C6}$–O–(C=O)–CH_3), 63.1 (HO–Ph–CH_2–$\underline{CH}$(–NH–C6)–(C=O)–O–CH_3) and, 69.0–81.5 ($\underline{C2}$, $\underline{C3}$, $\underline{C4}$, $\underline{C5}$), 99.4 and 103.0 ($\underline{C1}$), 115.0, 127.6, 130.1 and 155.8 (HO–$\underline{Ph}$–CH_2–CH(–NH–C6)–(C=O)–O–CH_3), 168.8–170.5 (O–($\underline{C}$=O)–CH_3), 174.5 (HO–Ph–CH_2–CH(–NH–C6)–($\underline{C}$=O)–O–CH_3). Elemental analysis: C 50.78%, H 5.86%, N 1.64%, I 4.04%; theoretical (DS(Ac) 1.78, DS(tyrosine ester) 0.37, DS(I) 0.1): C 50.75%, H 5.63%, N 1.65%, I 4.04% (note that there is some residual halogen and some of it is iodide via bromide displacement; measured as iodide).

2.2.4. Synthesis of proline tert-butyl ester- substituted cellulose acetate (6-ProCA320S)

6-BrCA320S (150 mg, 0.56 mmol) was dissolved in 10 mL DMSO in a 100 mL round-bottom flask. Proline *tert*-butyl ester (1.45 mL, 1.45 g, density 0.995 g/cm^2, 8.45 mmol, 15 equiv per AGU) and sodium iodide (169 mg, 1.13 mmol, 2 equiv per AGU) were added to the flask. The solution was kept at 80 °C with stirring for 48 h under N_2. The cooled solution was dialyzed against acetone for 7 days, then against DI-water for 2 days. The mixture was freeze-dried to yield 6-ProCA320S as light yellow powder. Yield: 141 mg, 0.46 mmol, 81%. ^{1}H NMR (400 MHz, DMSO-d_6) 1.47 ((N–C6)–CH_2–CH_2–CH_2–CH–(C=O)–O–C($\underline{CH_3}$)$_3$), 1.69–2.28 (O–(C=O)–$\underline{CH_3}$, (N–C6)–CH_2–$\underline{CH_2}$–CH_2–CH–(C=O)–O–C(CH_3)$_3$, and (N–C6)–CH_2–CH_2–$\underline{CH_2}$–CH–(C=O)–O–C(CH_3)$_3$), 2.42 ((N–C6)–CH_2–CH_2–$\underline{CH_2}$–CH–(C=O)–O–C(CH_3)$_3$), 2.72–5.37 (cellulose backbone, (N–C6)–$\underline{CH_2}$–CH_2–CH_2–CH–(C=O)–O–C(CH_3)$_3$, and (N–C6)–CH_2–CH_2–CH_2–$\underline{CH}$–(C=O)–O–C(CH_3)$_3$). ^{13}C NMR (500 MHz, DMSO-d_6) 20.5 (O–(C=O)–$\underline{CH_3}$), 23.4 ((N–C6)–CH_2–$\underline{CH_2}$–CH_2–CH–(C=O)–O–C(CH_3)$_3$), 27.8 ((N–C6)–CH_2–CH_2–CH_2–CH–(C=O)–O–C($\underline{CH_3}$)$_3$), 29.6 ((N–C6)–CH_2–CH_2–$\underline{CH_2}$–CH–(C=O)–O–C(CH_3)$_3$), 52.9 ($\underline{C6}$–N) and ((N–C6)–$\underline{CH_2}$–CH_2–CH_2–CH–(C=O)–O–C(CH_3)$_3$), 62.5 ($\underline{C6}$–O–(C=O)–CH_3), 65.4 and 66.4 ((N–C6)–CH_2–CH_2–CH_2–$\underline{CH}$–(C=O)–O–C(CH_3)$_3$), 69.0–81.5 ($\underline{C2}$, $\underline{C3}$, $\underline{C4}$, $\underline{C5}$), 79.7 ((N–C6)–CH_2–CH_2–CH_2–CH–(C=O)–O–$\underline{C}$(CH_3)$_3$), 99.4 and 102.8 ($\underline{C1}$), 168.5–170.4 (O–($\underline{C}$=O)–CH_3), 173.4 ((N–C6)–CH_2–CH_2–CH_2–CH–($\underline{C}$=O)–O–C(CH_3)$_3$). Elemental analysis: C 52.14%, H 6.61%, N 2.03%, I 0.89%; theoretical (DS(Ac) 1.78, DS (proline ester) 0.45, DS (I) 0.02): C 53.00%, H 6.63%, N 2.04%, I 0.82%.

2.2.5. Synthesis of 6-Boc-histidine methyl ester-substituted cellulose acetate (6-HisCA320S)

In a 100 mL round-bottom flask, 6-BrCA320S (150 mg, 0.56 mmol) was dissolved in DMSO (10 mL). N_α,N_{im}-di-Boc-L-histidine methyl ester (3.12 g, 8.45 mmol, 15 equiv per AGU) and sodium iodide (169 mg, 1.13 mmol, 2 equiv per AGU) were added to the flask. The solution was kept at 80 °C with stirring for 48 h under N_2. The cooled solution was dialyzed against acetone for 7 days, then against DI-water for 2 days. The mixture was freeze-dried to yield 6-HisCA320S as light yellow powder. Yield: 126 mg, 0.41 mmol, 73%. ^{1}H NMR (400 MHz, DMSO-d_6) 1.34 (N=CH–(N–C6)–CH=C–CH_2–CH(–NH–(C=O)–O–C($\underline{CH_3}$)$_3$)–(C=O)–O–CH_3), 2.03 (O–(C=O)–$\underline{CH_3}$), 2.80–5.47 (cellulose backbone, N=CH–(N–C6)–CH=C–$\underline{CH_2}$–CH(–NH–(C=O)–O–C(CH_3)$_3$)–(C=O)–O–CH_3, N=CH–(N–C6)–CH=C–CH_2–$\underline{CH}$(–NH–(C=O)–O–C(CH_3)$_3$)–(C=O)–O–CH_3, and N=CH–(N–C6)–CH=C–CH_2–CH(–NH–(C=O)–O–C(CH_3)$_3$)–(C=O)–O–$\underline{CH_3}$), 7.38 (N=CH–(N–C6)–$\underline{CH}$=C–CH_2–CH(–NH–(C=O)–O–C(CH_3)$_3$)–(C=O)–O–CH_3), 8.92 (N=$\underline{CH}$–(N–C6)–CH=C–CH_2–CH(–NH–(C=O)–O–C(CH_3)$_3$)–(C=O)–O–CH_3). ^{13}C NMR (500 MHz, DMSO-d_6) 20.6 (O–

(C=O)–CH$_3$), 28.2 (N=CH–(N–C6)–CH=C–CH$_2$–CH(–NH–(C=O)–O–C(CH$_3$)$_3$)–(C=O)–O–CH$_3$), 29.5 (N=CH–(N–C6)–CH=C–CH$_2$–CH(–NH–(C=O)–O–C(CH$_3$)$_3$)–(C=O)–O–CH$_3$), 46.4 (C6–N), 51.8 (N=CH–(N–C6)–CH=C–CH$_2$–CH(–NH–(C=O)–O–C(CH$_3$)$_3$)–(C=O)–O–CH$_3$), 53.8 (N=CH–(N–C6)–CH=C–CH$_2$–CH(–NH–(C=O)–O–C(CH$_3$)$_3$)–(C=O)–O–CH$_3$), 62.5 (C6–O–(C=O)–CH$_3$), 69.0–81.5 (C2, C3, C4, C5), 78.4 (N=CH–(N–C6)–CH=C–CH$_2$–CH(–NH–(C=O)–O–C(CH$_3$)$_3$)–(C=O)–O–CH$_3$), 99.3 and 102.8 (C1), 117.7 (N=CH–(N–C6)–CH=C–CH$_2$–CH(–NH–(C=O)–O–C(CH$_3$)$_3$)–(C=O)–O–CH$_3$), 136.8 and 137.4 (N=CH–(N–C6)–CH=C–CH$_2$–CH(–NH–(C=O)–O–C(CH$_3$)$_3$)–(C=O)–O–CH$_3$) and (N=CH–(N–C6)–CH=C–CH$_2$–CH(–NH–(C=O)–O–C(CH$_3$)$_3$)–(C=O)–O–CH$_3$), 155.2 (N=CH–(N–C6)–CH=C–CH$_2$–CH(–NH–(C=O)–O–C(CH$_3$)$_3$)–(C=O)–O–CH$_3$), 168.7–170.6 (O–(C=O)–CH$_3$), 172.5 (N=CH–(N–C6)–CH=C–CH$_2$–CH(–NH–(C=O)–O–C(CH$_3$)$_3$)–(C=O)–O–CH$_3$). Elemental analysis: C 47.54%, H 5.63%, N 2.98%, I 2.14; theoretical (DS (Ac) 1.78, DS(proline ester) 0.22, DS(I) 0.05): C 47.22%, H 5.54%, N 2.98%, I 2.04%.

2.2.6. Synthesis of 6-tyrosine tert-butyl ester-substituted dextran (6-TyrDextran)

6-BrDextran (200 mg, 1.17 mmol) was dissolved in 10 mL DMSO in a 100 mL round-bottom flask. Tyrosine *tert*-butyl ester (475 mg, 2.00 mmol, 12.9 equiv per non-reducing end) and NaI (120 mg, 0.80 mmol, 5.2 equiv per non-reducing end) were added to the flask. The solution was heated to 80 °C with stirring for 48 h under N_2. The cooled solution was dialyzed against 33% acetone, acetone, and water in sequence; the sequence was repeated several times, for a total of 28 days. Then, the mixture was freeze-dried to yield 6-TyrDextran as a brown fibrous material. Yield: 27 mg, 0.15 mmol, 13%. ^{1}H NMR (500 MHz, DMSO-d_6) 1.24 (HO–Ph–CH$_2$–CH(–NH–C6)–(C=O)–O–(CH$_3$)$_3$), 2.90–5.11 (dextran backbone, HO–Ph–CH$_2$–CH(–NH–C6)–(C=O)–O–(CH$_3$)$_3$, and HO–Ph–CH$_2$–CH(–NH–C6)–(C=O)–O–(CH$_3$)$_3$), 6.71 and 7.01 (HO–Ph–CH$_2$–CH

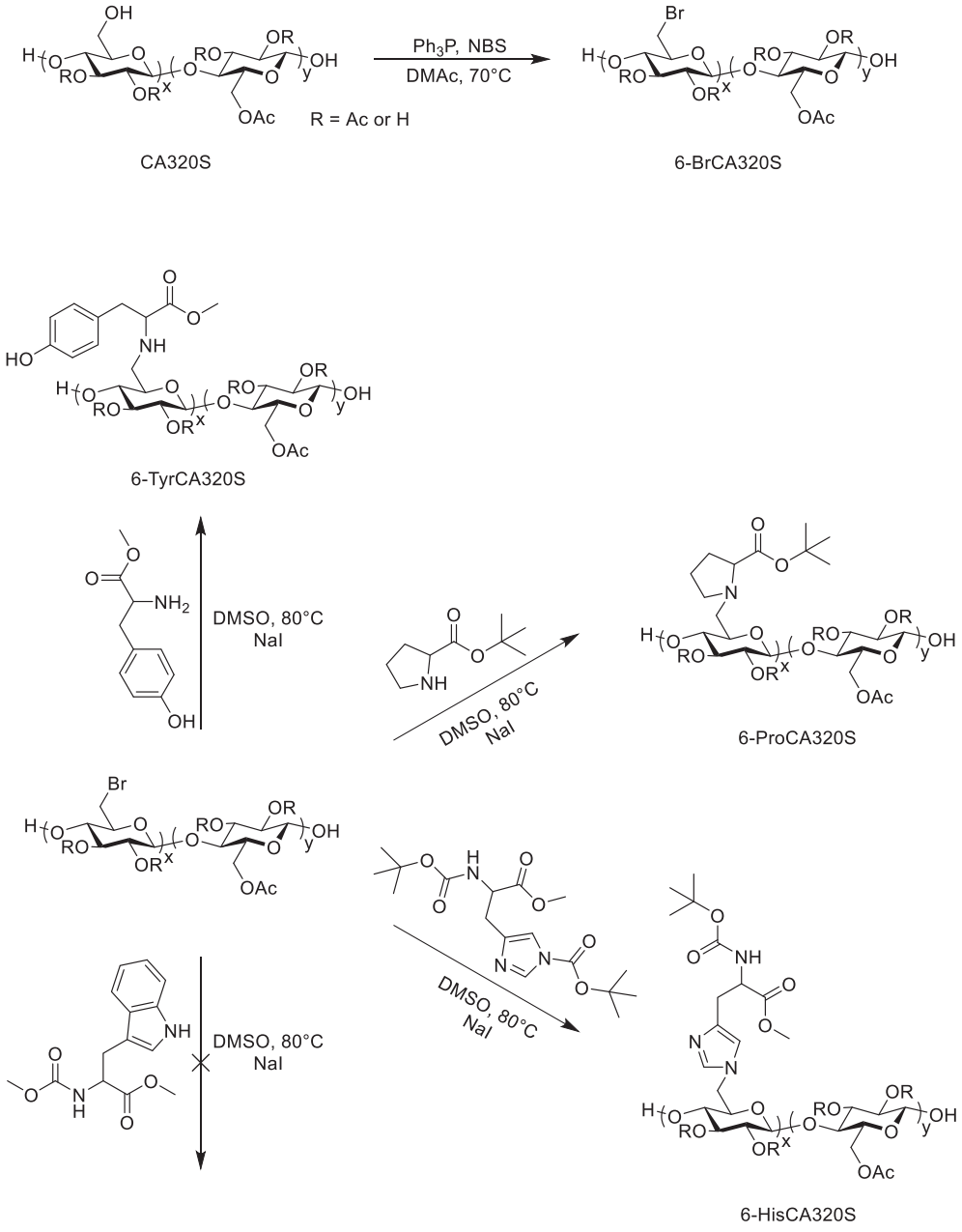

Scheme 1. Reaction scheme of regioselective bromination of CA320S followed by S_N2 reaction with tyrosine ester, proline ester, histidine ester, and tryptophan ester.

(–NH–C6)–(C=O)–O–$(CH_3)_3$).

2.2.7. Synthesis of proline tert-butyl ester-substituted dextran (6-ProDextran)

6-BrDextran (200 mg, 1.17 mmol) was dissolved in DMSO (10 mL) in a 100 mL round-bottom flask. Proline *tert*-butyl ester (344 μL, 342 mg, density 0.995 g/cm^2, 2.00 mmol, 12.9 equiv per non-reducing end) and sodium iodide (120 mg, 0.80 mmol, 5.2 equiv per non-reducing end) were added to the flask. The solution was heated to 80 °C with stirring for 48 h under N_2. The cooled solution was dialyzed against 33% acetone, acetone, and water in sequence; the sequence was repeated several times for a total of 28 days. Then, the mixture was freeze-dried to yield 6-ProDextran as a brown fibrous material. Yield: 26 mg, 0.14 mmol, 12%. ^{1}H NMR (500 MHz, DMSO-d_6) 1.24 ((N–C6)–CH_2–CH_2–CH_2–CH–(C=O)–O–C(CH_3)$_3$), 1.50–2.50 ((N–C6)–CH_2–CH_2–CH_2–CH–(C=O)–O–C$(CH_3)_3$, and (N–C6)–CH_2–CH_2–CH_2–CH–(C=O)–O–C$(CH_3)_3$), 2.90–5.11 (dextran backbone, (N–C6)–CH_2–CH_2–CH_2–CH–(C=O)–O–C$(CH_3)_3$, and (N–C6)–CH_2–CH_2–CH_2–CH–(C=O)–O–C$(CH_3)_3$).

3. Results and discussion

3.1. Reactions of 6-BrCA320S with amino acid esters

In our work, the commercial cellulose acetate CA320S was selected (see Scheme 1). It has a relatively high DS(6-OH) (roughly 0.5) available for selective bromination (Liu & Edgar, 2017). The brominated product, 6-BrCA320S, has good solubility in DMSO, which is a polar aprotic solvent favoring S_N2 reaction. However, amino acids tend to have low solubility in common organic solvents because of their zwitterionic character (Needham et al., 1971). Zwitterionic amino acids contain both ammonium and carboxylate groups and therefore have large dipole moments (Shao & Jiang, 2015). The protonated ammonium group will of course also have suppressed nucleophilicity. Therefore, we chose to employ amino acid esters in this initial study, rather than amino acids themselves. With the amino acid carboxyl groups converted to esters, these esters have much improved solubility in common organic solvents like DMSO and acetone, in addition to resolving the nucleophilicity issue since no carboxyl is available to protonate the amines.

3.1.1. 6-BrCA320S

The cellulose acetate used in this work had DS(6-OH) 0.49, measured by proton NMR spectroscopy of the perpropionylated derivative (Gao & Edgar, 2018; Liu & Edgar, 2017). Furuhata bromination (Furuhata et al., 1992) of this cellulose acetate using Liu's procedure (Ph_3P/NBS/DMAc, 70 °C, 1 h) afforded nearly quantitative conversion of the available 6-OH groups to 6-Br, with measured DS(Br) of 0.47 by elemental analysis. Excess triphenyl phosphine and byproduct triphenylphosphine oxide can be difficult to remove completely from the bromination product (Fox & Edgar, 2012; Zhang & Edgar, 2014), but none were detected in CA320S-based conjugates. A small amount of residual DMF was revealed by the low N content detected via elemental analysis, but it did not interfere with subsequent steps. The new ^{13}C resonance at 37 ppm was diagnostic, and was assigned to bromo-substituted C6 (Fig. S1), consistent with Liu's observations (Liu & Edgar, 2017).

3.1.2. 6-TyrCA320S

Gao reported that 6-chloro-6-deoxycellulose esters (6-ClCA320S) underwent nucleophilic chloride displacement by *n*-butylamine in DMSO at 70 °C in the presence of NaI, to generate transient concentrations of the better alkyl iodide leaving group (Gao et al., 2018). Unfortunately, we found that reaction of 6-ClCA320S with tyrosine ester in DMSO at 80 °C with added NaI did not afford satisfactory conversion to the amino acid adduct, presumably due to the fact that the amino acid ester is a weaker nucleophile than *n*-butylamine. Therefore, we investigated displacements using amino acid esters with 6-BrCA320S containing the superior bromide leaving group.

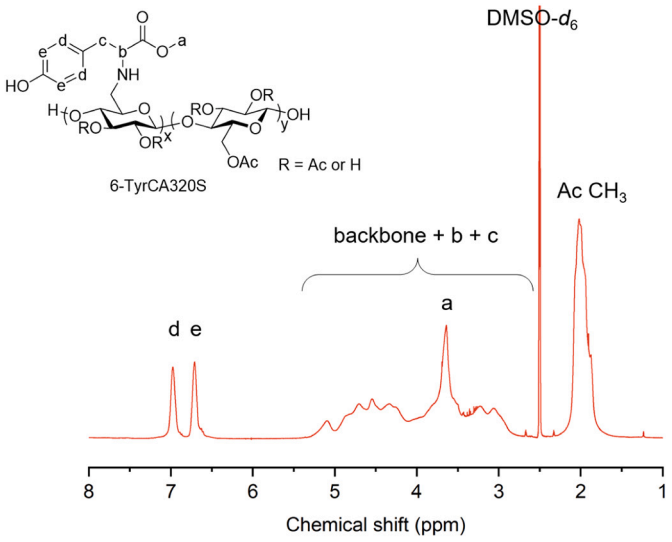

Fig. 1. ^{1}H NMR spectrum of 6-TyrCA320S.

Tyrosine methyl ester was useful for initial experiments, since its phenol ring has downfield ^{1}H NMR resonances (6.5–7 ppm), readily distinguished and integrated from the more upfield resonances of the starting cellulose derivative. Reaction at 80 °C for 48 h in the presence of NaI afforded a product that was readily isolated by dialysis. In its ^{1}H NMR spectrum (Fig. 1), we assigned the sharp peak at about 3.6 ppm to the methyl group from the appended tyrosine ester. New resonances appeared at 6.6–7.1 ppm from the ortho and meta protons of the tyrosine phenol ring. DS(tyrosine ester) was 0.36, as calculated from the ratios of either set of peaks to the backbone protons in the ^{1}H spectrum. Based on the DS(Br) of the starting cellulose derivative, the conversion was 77%. DS and conversion were also confirmed by elemental analysis of the product, which afforded a nearly identical DS(tyrosine ester) value of 0.37. There was no evidence of DMF or DMAc residue in the product ^{1}H NMR spectrum, supporting the hypothesis that all product nitrogen content results from the appended amino acid ester. There was some concern that reacting with an amino acid ester under these conditions might result in some deacylation of the halogenated cellulose acetate starting material, by reaction with the basic and nucleophilic amine (Gao et al., 2018). However, the product DS(Ac) as measured by ^{1}H NMR integration held steady at 1.78, indicating that no measurable deacetylation occurred during reaction with the amino acid ester.

We further confirmed the structure of 6-TyrCA320S by ^{13}C NMR spectroscopy (Fig. 2). The former bromo-substituted C6 at 37 ppm was absent in the product spectrum, while a new peak at 46 ppm was assigned to the tyrosine ester-substituted C6, consistent with Liu's and Zhang's observations (Liu & Edgar, 2017; Zhang & Edgar, 2014). The tyrosine methyl ester α-carbon at 56 ppm shifted downfield to 63 ppm in the 6-TyrCA320S product. These chemical shift changes strongly support the formation of the adduct C—N bond. No free tyrosine methyl ester was observed by ^{13}C NMR, nor were conjugates linked via the phenol observed; these would be expected to show an α-carbon ^{13}C resonance similar to that of starting tyrosine methyl ester (~56 ppm).

While conversion was not complete, this was an encouraging result, supporting selective 6-substitution on the polysaccharide, and participation exclusively by the α-amine, so we proceeded to explore the generality of the reaction.

3.1.3. 6-ProCA320S

It was expected that conjugation of the polysaccharide with a secondary amine would be more difficult, for approach angle reasons. Indeed, unlike most other natural amino acids, the α-amine of proline is a secondary amine as part of a five-membered ring; thus it was expected

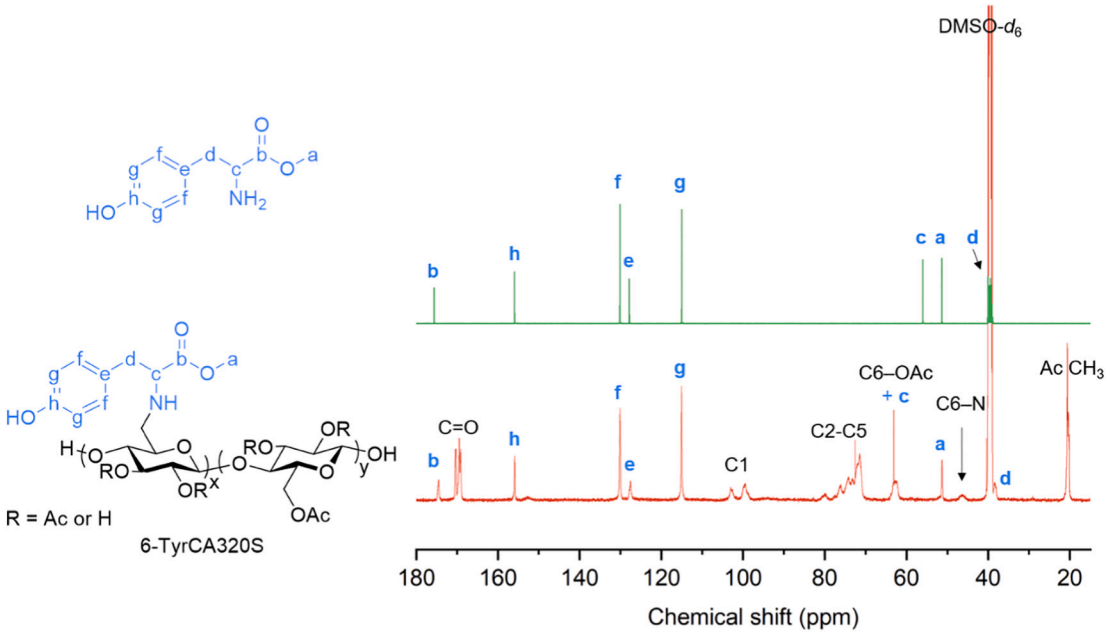

Fig. 2. ^{13}C NMR spectra of tyrosine methyl ester and 6-TyrCA320S.

to be instructive to test its utility in this displacement chemistry. We employed the *tert*-butyl ester of proline, in part because the *tert*-butyl group has a distinctive ^{1}H NMR resonance at around 1.4 ppm, cleanly separated from polysaccharide backbone resonances. In the event, reaction of 6-BrCA320S with tyrosine *tert*-butyl ester under conditions similar to those used with the proline ester afforded the desired tyrosine ester adduct, with DS(tyrosine ester) of 0.45 as calculated by ^{1}H NMR spectrum integration, and confirmed by elemental analysis. Interestingly, conversion of 6-BrCA320S was higher when reacting with the secondary amine, proline t-butyl ester (96%), than with the primary amine, tyrosine methyl ester (77%). This somewhat surprising result is likely due to the fact that the proline amine is part of a pyrrolidine ring and thus has wide approach angles; thus pyrrolidine has a higher nucleophilic reactivity than the acyclic isopropylamine (Kanzian et al., 2009). There was no evidence for deacetylation during the displacement reaction, even though proline amine (pKa 10.64), in addition to being a better nucleophile, is a stronger base than is tyrosine amine (pKa 9.11) (Lide, 2004).

The proline adduct structure was confirmed by ^{13}C NMR spectroscopy (Fig. 3). Carbons d, g, and f from the pyrrolidine had new chemical shifts after conjugation. Carbon f, β to the amine, shifted upfield from 25 to 23 ppm; while those α to the amine shifted downfield; carbon g from 46 to 53 ppm; and carbon d from 60 to 66 ppm. The L-proline ester moiety was racemized to a D, L-mixture during the displacement reaction, as indicated by the two resonances observed for the amine-bearing carbon near 66 ppm. The C6–Br at 37 ppm disappeared, replaced by the new C6–N at 53 ppm, partly overlapped by the carbon g resonance. We investigated whether the resonances of carbon g and C6–N indeed

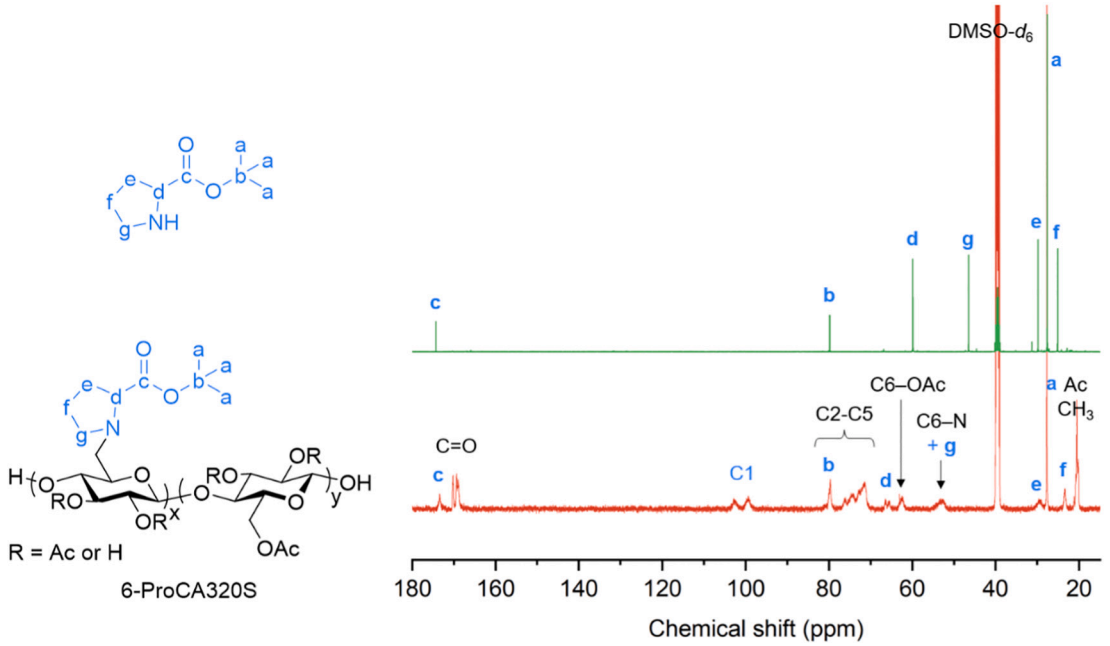

Fig. 3. ^{13}C NMR spectra of proline *tert*-butyl ester and 6-ProCA320S.

overlapped in the broad peak at 53 ppm by heteronuclear single quantum coherence (HSQC) analysis (Fig. S8). The resonance(s) at 53 ppm are correlated with two non-equivalent hydrogen, at roughly 2.6 ppm and 2.95 ppm. Of course, the C6 carbon resonance should itself be correlated with the two diastereotopic hydrogen at C6.

3.1.4. 6-HisCA320S

tert-Butoxycarbonyl (Boc) is a common amine protecting group in organic chemistry. We wished to test whether the tertiary amine in histidine could react with 6-BrCA320S, pushing the envelope still further, so we elected to use the protected histidine derivative, N_{α}, N_{im}-di-Boc-L-histidine methyl ester, hoping to avoid competition from its primary and secondary amine moieties (Fig. 4). To our surprise, the tertiary (85 ppm) and ester (147 ppm) carbons of the Boc group protecting the secondary amine in histidine disappeared after conjugation, while the Boc-protecting group of the primary amine was still present, as determined by ^{13}C NMR analysis. Even though the signal-to-noise ratio was relatively low in the ^{13}C NMR spectra of the starting material and this derivative, the three equivalent methyls in each Boc functional group provided observable resonances. We observed two methyl resonances from the two Boc groups in the starting histidine ester, but only one resonance remained after condensation. We were also able to identify the histidine ester reaction site as being the deprotected amine. As with the tyrosine ester and proline ester conjugates, for the histidine ester conjugate the C6–Br carbon resonance disappeared and a C6–N resonance at 46 ppm appeared. Carbon i in the imidazole ring moved upfield from 137 to 118 ppm, while ring carbon h moved downfield from 114 to 137 ppm. Imidazole carbon j shifted only slightly from 139 to 137 ppm. The aromatic imidazole nitrogen is expected to be more weakly nucleophilic than tyrosine or proline amines (Bentley, 2011). Addition of TFA to the polysaccharide solution, typically useful for moving water resonances downfield and out of the integral area of interest, in this case caused a change in the values of integrals of imidazole protons, therefore we calculated DS(histidine ester) using the ratio of Boc protons to backbone by ^{1}H NMR (Fig. S3). DS(histidine ester) was 0.23, and this value was confirmed by elemental analysis. It was clear by ^{1}H NMR spectroscopy that no significant deacetylation had occurred, consistent with the weaker histidine nucleophilicity.

3.1.5. Reacting 6-BrCA320S with tryptophan ester

N_{α}-methoxycarbonyl-L-tryptophan methyl ester also contains a secondary amine, but it is appended to the side chain rather than the α-amine; therefore this also would be an illustrative substrate. Upon reaction of 6-BrCA320S with tryptophan ester at 80 °C in DMSO, the isolated product exhibited no ^{1}H NMR resonances assignable to the indole ring of tryptophan; no significant deacetylation occurred. The indole structure is highly stable (Pino-Rios & Solà, 2020); extensive delocalization of the nitrogen lone pair of nitrogen reduces its nucleophilicity (Anderson & Liu, 2000). Kleinschek et al. also concluded that the α-amine of L-tryptophan methyl ester can react with carboxyls via EDC coupling, but the amine at its side chain cannot (Gürer et al., 2021).

3.2. Reactions of 6-BrDextran with amino acid esters

We were also interested in exploring conjugation to the polysaccharide linear dextran, which also has good solubility in DMSO (see Scheme 2). Dextran consists of an α-(1,6)-linked glucan main chain, which depending on the bacterium that produces it, may have α-glucose branches emanating from any of the secondary alcohol positions (Zohuri, 2012). Linear dextran is of particular interest since it is regularly administered intravenously to patients, and can be cleared from the body by enzymatic degradation and filtration through the kidneys, therefore toxicity and clearance for biomedical applications are extremely unlikely to be problematic (Mehvar, 2000). Because of its α-1-6 linkages, there is one and only one free primary hydroxyl group on the linear dextran backbone (except for those at termini of branches, if any), the 6-OH of the non-reducing end glucose monosaccharide. This presents the opportunity to synthesize linear adducts; of a certain interest with regard to amino acid adducts, and potentially of particular interest for polypeptide or protein adducts.

Since only the single 6-OH in the linear dextran backbone or branch is available, it is at low concentration; we calculated DS(C6-OH) = 0.132 by the integral ratio of resonances of H1 α(1,3) and H1 α(1,6) in its ^{1}H NMR spectrum (Fig. S4). We chose low DP dextran with molecular weight 10 kDa to maximize the proportion of non-reducing monosaccharides to the bulk of the polymer chain, while realizing that a downside of this approach is likely to be lower isolated yields due to loss

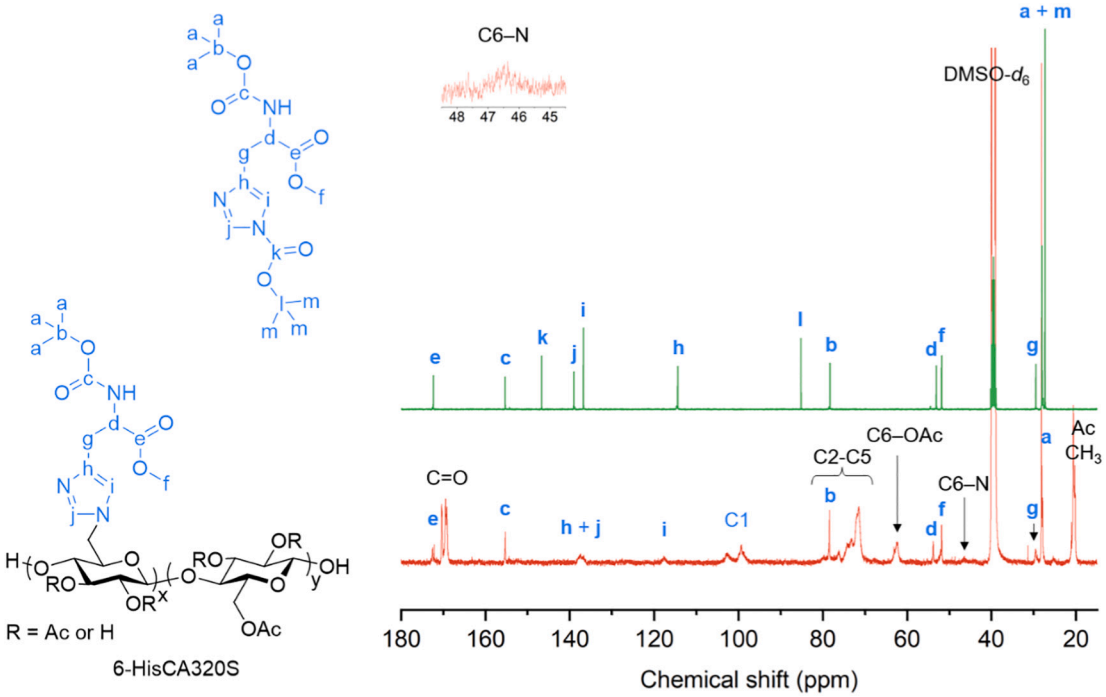

Fig. 4. ^{13}C NMR spectra of N_{α}, N_{im}-di-Boc-L-histidine methyl ester and 6-HisCA320S.

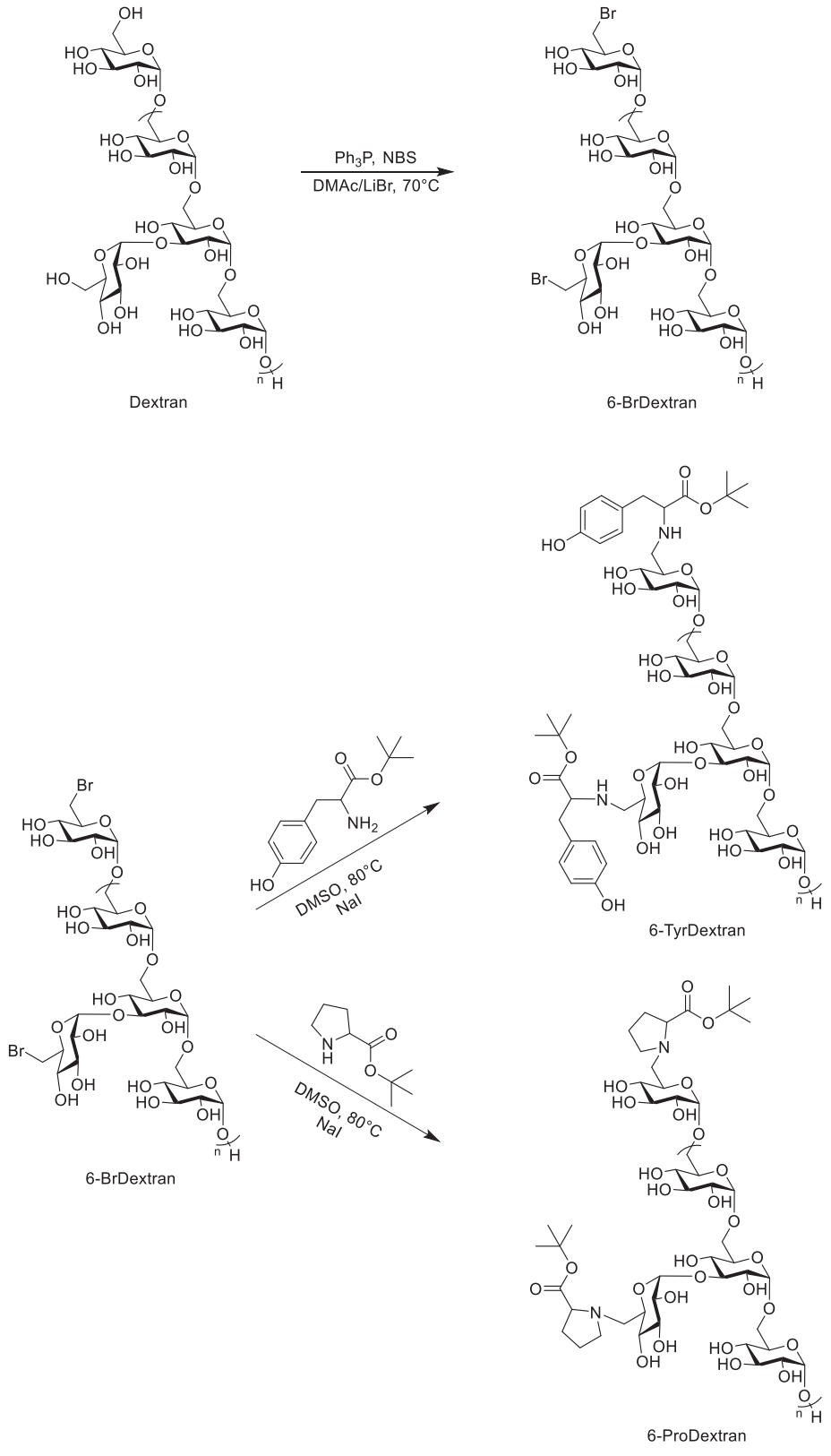

Scheme 2. Reaction scheme of regioselective bromination of dextran followed by S_N2 reaction with tyrosine ester or proline ester.

of the low DP end of the distribution during product dialysis. To improve our ability to detect and quantify the expected single amino acid ester moiety in the dextran-amino acid ester conjugate, we employed a *tert*-butyl ester of the amino acid substrate, reasoning that the nine proton singlet in the proton NMR would be helpful in that regard.

3.2.1. 6-BrDextran

Chen recently reported a method for brominating the available 6-OH at the non-reducing terminus of linear dextran, using Ph_3P/NBS in DMSO (Chen et al., 2020). However, reactions of NBS in DMSO can be plagued by side reactions, for example rapidly affording a bromine-containing sulfur cation, consuming NBS (Wu et al., 2020). We therefore carried out Ph_3P/NBS bromination of dextran in the DMAc/LiBr solvent system, observing no off-target bromination.

3.2.2. 6-TyrDextran

First, we selected tyrosine *tert*-butyl ester to conjugate to 6-BrDextran (Fig. S5). It has slightly larger steric bulk than the methyl ester used earlier in this work, but this is not expected to significantly impede the desired S_N2 displacement since the bulky *tert*-butyl group is sufficiently distant from the reaction site. The product ^{1}H NMR spectrum (Fig. 5) displays two clear resonances at 6.7 and 7.0 ppm, assigned to the phenyl ring protons of the appended tyrosine moiety. Resonances at 1.1–1.5 ppm were clear indications of the retained *tert*-butyl ester. The TFA added to the NMR sample in order to move the signal of free dextran hydroxyls and water downfield led to broad appearance of the *tert*-butyl resonance, as compared to the ^{1}H NMR spectrum without TFA (Fig. S6). The DS(tyrosine ester) calculated by integration of the ^{1}H NMR spectrum was 0.094, indicating 71% conversion of the available C6 hydroxyls.

3.2.3. 6-ProDextran

We also explored conjugation of proline *tert*-butyl ester with linear dextran (Fig. 6). Because proline does not possess an aromatic ring as does tyrosine, the side chain resonances in the product ^{1}H NMR spectrum are more diffuse and less distinct (remembering that they come from amino acid ester moieties at the non-reducing end C6 of the linear dextran chain). The *tert*-butyl resonance is most diagnostic for the desired conjugation, although again the addition of TFA led to a broad *tert*-butyl resonance (Fig. S7). The pyrrolidine proton resonances are broad and weak, but appear from 1.5–2.5 ppm, and can be assigned to protons c and d. The ratio of the *tert*-butyl resonance to the backbone protons indicated that the DS(proline ester) was 0.099, meaning that 75% of the available C6 hydroxyls were converted through the bromide to the *tert*-butyl proline ester substituent. 6-TyrDextran and 6-ProDextran are only partially soluble in water (Table S2), while dextran itself is soluble in water.

4. Conclusions

In this work, a synthetic strategy for preparing polysaccharide-amino acid ester conjugates has been developed, by employing 6-Br-polysaccharides in S_N2 substitution reactions with amino acid esters. Reaction of 6-BrCA320S with tyrosine methyl ester and proline *tert*-butyl ester, both in high conversion, showed that displacements with both primary amine and secondary amines at the amino acid α-carbon can be successful. Reacting with proline *tert*-butyl ester (96%) afforded a higher conversion compared to tyrosine methyl ester (77%), initially surprising to us but likely well explained by the different geometries of the two amino acid esters. In all cases, ester substituents on the polysaccharide were unmolested by the amino acid. We examined the situation in which the amino acid ester has amine-containing α-substituents by investigating condensation of 6-BrCA320S with tryptophan and histidine esters. Reaction with a tryptophan ester in which the α-amine was protected, thus forcing reaction to the indole nitrogen, was not successful, while the histidine side group gave successful displacement of the cellulose acetate 6-Br groups, but with relatively low conversion (49%). We also demonstrated that this strategy can be used to synthesize linear adducts by bromination of the free 6-OH group of dextran, followed by amino acid ester displacement of the bromide. Following regio- and chemoselective bromination of dextran 6-OH in DMAc/LiBr system, we observed high conversion displacements by the *tert*-butyl esters of tyrosine and proline, and were able to overcome the characterization issues caused by the low maximum possible degree of

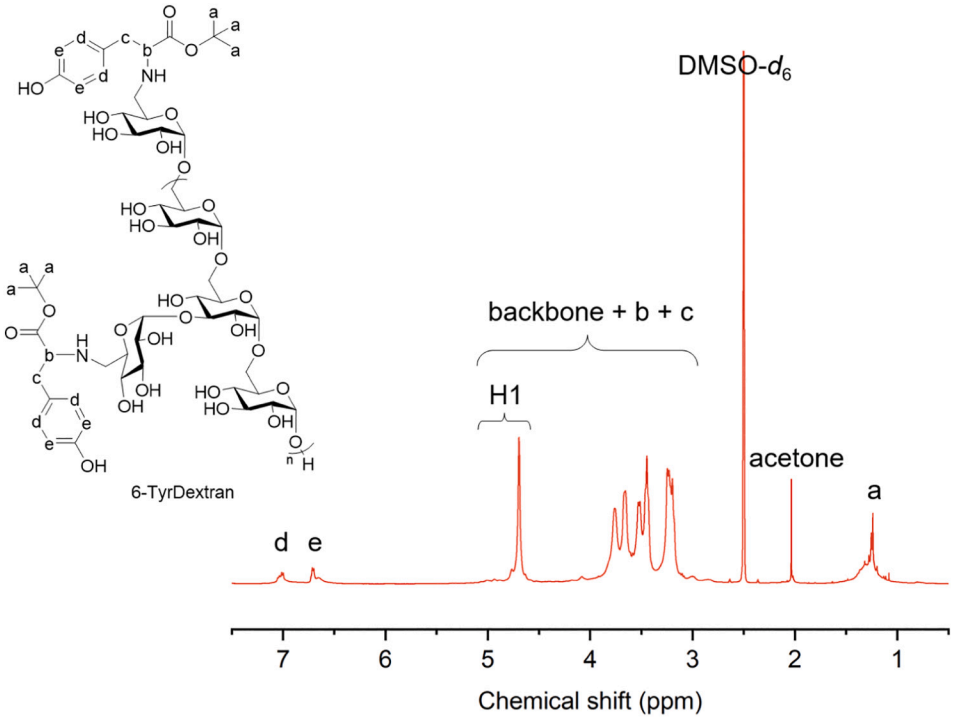

Fig. 5. ^{1}H NMR spectrum of 6-TyrDextran in the presence of TFA.

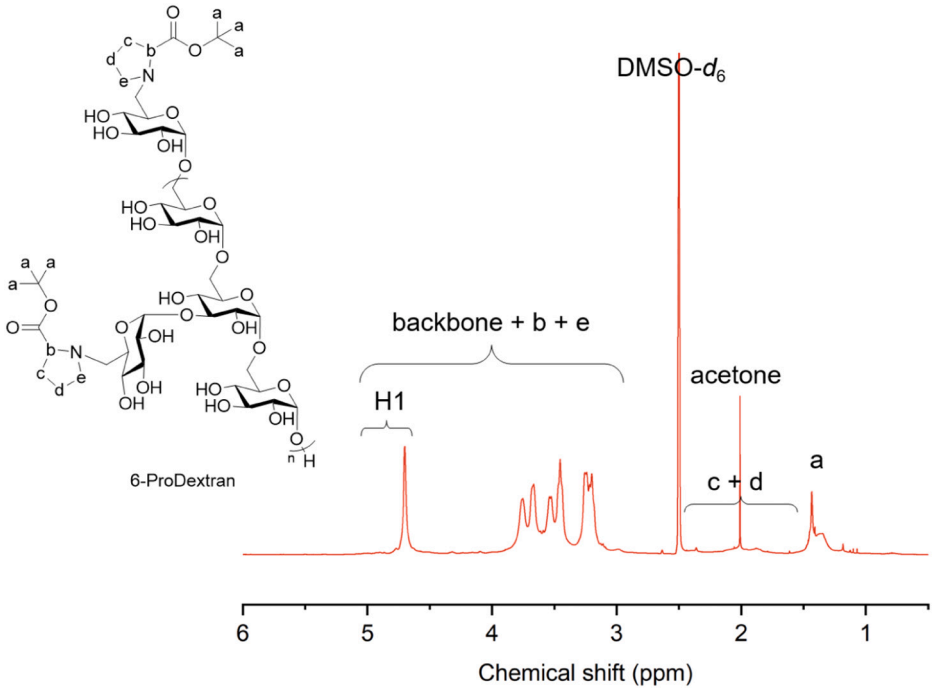

Fig. 6. ^{1}H NMR spectrum of 6-ProDextran in the presence of TFA.

substitution on the entire molecule.

Overall, this strategy promises to be widely applicable for regioselective decoration of polysaccharides with amino acid ester moieties. These adducts may themselves show interesting bioactivity, and utility in other applications. Perhaps more importantly, this polysaccharide–amino acid conjugation chemistry provides a good starting point for selective, efficient polysaccharide conjugation with proteins or polypeptides. We will describe our efforts to realize the possibility of such promising extensions in future reports.

CRediT authorship contribution statement

Yang Zhou: conception, design, visualization, drafting, and critical revisions. **Kevin J. Edgar**: conception, critical revisions, and supervision.

Declaration of competing interest

The authors report no competing interests.

Acknowledgements

We thank the Virginia Tech Institute for Critical Technology and Applied Science, the Department of Sustainable Biomaterials, and the College of Natural Resources and Environment for partial support of this work. We are thankful for the David W. Francis & Lillian Francis Research Fellowship (YZ) which provided partial support of this work. We thank the National Science Foundation (PFI-RP) for partial support of this work through grant IIP-1827493. We thank Professors Young-Teck Kim and Patricia Dove for access to lyophilizers; as well as Soo-hyung Lee and Austin Fergusson for training on them.

Appendix A. Supplementary data

Supplementary data to this article can be found online at https://doi.org/10.1016/j.carbpol.2021.118886.

References

Anderson, L. R., & Liu, K. C. (2000). Pyrrole and pyrrole derivatives. *Kirk-Othmer Encyclopedia of Chemical Technology*. https://doi.org/10.1002/0471238961.1625181801140405.a01

Baumann, A., Tuerck, D., Prabhu, S., Dickmann, L., & Sims, J. (2014). Pharmacokinetics, metabolism and distribution of PEGs and PEGylated proteins: Quo vadis? *Drug Discovery Today, 19*(10), 1623–1631. https://doi.org/10.1016/j.drudis.2014.06.002

Bentley, T. W. (2011). Nucleophilicity parameters for amines, amino acids and peptides in water. Variations in selectivities for quinone methides. *Organic & Biomolecular Chemistry, 9*(19), 6685–6690. https://doi.org/10.1039/c1ob05715d

Buchanan, C. M., Gardner, R. M., & Komarek, R. J. (1993). Aerobic biodegradation of cellulose acetate. *Journal of Applied Polymer Science, 47*(10), 1709–1719. https://doi.org/10.1002/app.1993.070471001

Chen, J., Spiering, G., Mosquera-Giraldo, L., Moore, R. B., & Edgar, K. J. (2020). Regioselective bromination of the dextran nonreducing end creates a pathway to dextran-based block copolymers. *Biomacromolecules, 21*(5), 1729–1738. https://doi.org/10.1021/acs.biomac.9b01668

Damodaran, V. B., & Fee, C. (2010). Protein PEGylation: An overview of chemistry and process considerations. *European Pharmaceutical Review, 15*(1), 18–26.

Ferguson, E. L., Varache, M., Stokniene, J., & Thomas, D. W. (2020). Polysaccharides for protein and peptide conjugation. In *Polymer-protein conjugates* (pp. 421–453). Elsevier.

Fox, S. C., & Edgar, K. J. (2012). Staudinger reduction chemistry of cellulose: Synthesis of selectively O-acylated 6-amino-6-deoxy-cellulose. *Biomacromolecules, 13*(4), 992–1001. https://doi.org/10.1021/bm2017004

Furuhata, K.-i., Koganei, K., Chang, H.-S., Aoki, N., & Sakamoto, M. (1992). Dissolution of cellulose in lithium bromide-organic solvent systems and homogeneous bromination of cellulose with N-bromosuccinimide-triphenylphosphine in lithium bromide-N, N-dimethylacetamide. *Carbohydrate research, 230*(1), 165–177. https://doi.org/10.1016/S0008-6215(00)90519-6

Gao, C., & Edgar, K. J. (2018). Efficient synthesis of glycosaminoglycan analogs. *Biomacromolecules, 20*(2), 608–617. https://doi.org/10.1021/acs.biomac.8b01150

Gao, C., Liu, S., & Edgar, K. J. (2018). Regioselective chlorination of cellulose esters by methanesulfonyl chloride. *Carbohydrate Polymers, 193*, 108–118. https://doi.org/10.1016/j.carbpol.2018.03.093

Gürer, F., Kargl, R., Bračič, M., Makuc, D., Thonhofer, M., Plavec, J., & Kleinschek, K. S. (2021). Water-based carbodiimide mediated synthesis of polysaccharide-amino acid conjugates: Deprotection, charge and structural analysis. *Carbohydrate Polymers, 267*, Article 118226. https://doi.org/10.1016/j.carbpol.2021.118226

Heinze, T., Liebert, T., Heublein, B., & Hornig, S. (2006). Functional polymers based on dextran. *Polysaccharides Ii*, 199–291.

Hotzel, K., Zemljic, L. F., Bracic, M., & Heinze, T. (2019). Protonation behavior of dextran amino acid esters. *Turkish Journal of Chemistry, 43*(3), 869–880. https://doi.org/10.3906/kim-1901-12

Hu, Q., Lu, Y., & Luo, Y. (2021). Recent advances in dextran-based drug delivery systems: From fabrication strategies to applications. *Carbohydrate Polymers, 264*, Article 117999. https://doi.org/10.1016/j.carbpol.2021.117999

Huang, S., & Huang, G. (2019). Preparation and drug delivery of dextran-drug complex. *Drug Delivery, 26*(1), 252–261. https://doi.org/10.1080/10717544.2019.1580322

Huang, M., Chen, F., Jiang, Z., & Li, Y. (2013). Preparation of TEMPO-oxidized cellulose/amino acid/nanosilver biocomposite film and its antibacterial activity. *International Journal of Biological Macromolecules, 62*, 608–613. https://doi.org/10.1016/j.ijbiomac.2013.10.018

Jevševar, S., Kunstelj, M., & Porekar, V. G. (2010). PEGylation of therapeutic proteins. *Biotechnology Journal: Healthcare Nutrition Technology, 5*(1), 113–128. https://doi.org/10.1002/biot.200900218

Kanzian, T., Nigst, T. A., Maier, A., Pichl, S., & Mayr, H. (2009). *Nucleophilic reactivities of primary and secondary amines in acetonitrile*. https://doi.org/10.1002/ejoc.200900925

Kawai, F. (2005). Biodegradation of polyethers (polyethylene glycol, polypropylene glycol, polytetramethylene glycol, and others). In *, 9. Biopolymers Online: Biology• Chemistry• Biotechnology• Applications*. https://doi.org/10.1002/3527600035.bpol9012

Khoshnevisan, K., Maleki, H., Samadian, H., Shahsavari, S., Sarrafzadeh, M. H., Larijani, B., & Khorramizadeh, M. R. (2018). Cellulose acetate electrospun nanofibers for drug delivery systems: Applications and recent advances. *Carbohydrate Polymers, 198*, 131–141. https://doi.org/10.1016/j.carbpol.2018.06.072

Lide, D. R. (2004). *CRC handbook of chemistry and physics*. CRC Press.

Liu, S., & Edgar, K. J. (2017). Water-soluble co-polyelectrolytes by selective modification of cellulose esters. *Carbohydrate Polymers, 162*, 1–9. https://doi.org/10.1016/j.carbpol.2017.01.008

Mehvar, R. (2000). Dextrans for targeted and sustained delivery of therapeutic and imaging agents. *Journal of Controlled Release, 69*(1), 1–25. https://doi.org/10.1016/s0168-3659(00)00302-3

Naessens, M., Cerdobbel, A., Soetaert, W., & Vandamme, E. J. (2005). Leuconostoc dextransucrase and dextran: Production, properties and applications. *Journal of Chemical Technology & Biotechnology: International Research in Process, Environmental & Clean Technology, 80*(8), 845–860. https://doi.org/10.1002/jctb.1322

Needham, T., Jr., Paruta, A., & Gerraughty, R. (1971). Solubility of amino acids in pure solvent systems. *Journal of Pharmaceutical Sciences, 60*(4), 565–567. https://doi.org/10.1002/jps.2600600410

Pahlevan, M., Toivakka, M., & Alam, P. (2018). Mechanical properties of TEMPO-oxidised bacterial cellulose-amino acid biomaterials. *European Polymer Journal, 101*, 29–36. https://doi.org/10.1016/j.eurpolymj.2018.02.013

Pereira, J. M., & Edgar, K. J. (2014). Regioselective synthesis of 6-amino-and 6-amido-6-deoxypullulans. *Cellulose, 21*(4), 2379–2396. https://doi.org/10.1007/s10570-014-0259-6

Pino-Rios, R., & Solà, M. (2020). The relative stability of indole isomers is a consequence of the glidewell-Lloyd rule. *The Journal of Physical Chemistry A, 125*(1), 230–234. https://doi.org/10.1021/acs.jpca.0c09549

Roberts, M., Bentley, M., & Harris, J. (2012). Chemistry for peptide and protein PEGylation. *Advanced Drug Delivery Reviews, 64*, 116–127. https://doi.org/10.1016/j.addr.2012.09.025

Saito, T., & Isogai, A. (2004). TEMPO-mediated oxidation of native cellulose. The effect of oxidation conditions on chemical and crystal structures of the water-insoluble fractions. *Biomacromolecules, 5*(5), 1983–1989. https://doi.org/10.1021/bm0497769

Shao, Q., & Jiang, S. (2015). Molecular understanding and design of zwitterionic materials. *Advanced Materials, 27*(1), 15–26. https://doi.org/10.1002/adma.201404059

Sun, T., Xu, H., Zhang, H., Ding, H., Cui, S., Xie, J., & Hua, X. (2018). Maillard reaction of oat β-glucan and the rheological property of its amino acid/peptide conjugates. *Food Hydrocolloids, 76*, 30–34. https://doi.org/10.1016/j.foodhyd.2017.07.025

Touati, K., & Tadeo, F. (2017). Pressure retarded osmosis as renewable energy source. In *Pressure Retarded Osmosis* (pp. 1–54). Elsevier.

Varshosaz, J. (2012). Dextran conjugates in drug delivery. *Expert Opinion on Drug Delivery, 9*(5), 509–523. https://doi.org/10.1517/17425247.2012.673580

Wu, Y., Zhang, M., Zhang, Y., Li, M., Feng, W., Zheng, X., & Tang, L. (2020). NBS-activated cross-dehydrogenative esterification of carboxylic acids with DMSO. *Organic Chemistry Frontiers, 7*(18), 2719–2724. https://doi.org/10.1039/D0QO00617C

Yi, Y., Han, M.-M., Huang, F., Wang, L.-M., Min, T., & Wang, H.-X. (2019). Effects of a lysine-involved maillard reaction on the structure and in vitro activities of polysaccharides from longan pulp. *Molecules, 24*(5), 972. https://doi.org/10.3390/molecules24050972

Zhang, R., & Edgar, K. J. (2014). Synthesis of curdlan derivatives regioselectively modified at C-6: O-(N)-acylated 6-amino-6-deoxycurdlan. *Carbohydrate Polymers, 105*, 161–168. https://doi.org/10.1016/j.carbpol.2014.01.045

Zhang, R., Liu, S., & Edgar, K. J. (2017). Efficient synthesis of secondary amines by reductive amination of curdlan staudinger ylides. *Carbohydrate Polymers, 171*, 1–8. https://doi.org/10.1016/j.carbpol.2017.04.093

Zhou, Y., Petrova, S. P., & Edgar, K. J. (2021). Chemical synthesis of polysaccharide–protein and polysaccharide–peptide conjugates: A review. *Carbohydrate Polymers, 274*, Article 118662. https://doi.org/10.1016/j.carbpol.2021.118662

Zink, M., Hotzel, K., Schubert, U. S., Heinze, T., & Fischer, D. (2019). Amino acid-substituted dextran-based non-viral vectors for gene delivery. *Macromolecular Bioscience, 19*(8), 1900085. https://doi.org/10.1002/mabi.201900085

Zohuri, G. (2012). *Polymer science: a comprehensive reference*.